The Journal of Experimental Biology 208, 1915-1925
Published by The Company of Biologists 2005
doi:10.1242/jeb.01570

Genomic sequences encoding two types of medaka hemopexin-like protein Wap65, and their gene expression profiles in embryos

Makiko Nakaniwa[1], Makoto Hirayama[1], Atsushi Shimizu[2], Takashi Sasaki[2], Shuichi Asakawa[2], Nobuyoshi Shimizu[2] and Shugo Watabe[1,*]

[1]*Laboratory of Aquatic Molecular Biology and Biotechnology, Graduate School of Agricultural and Life Sciences, The University of Tokyo, Tokyo113-8657, Japan* and [2]*Department of Molecular Biology, Keio University School of Medicine, 35 Shinanomachi, Shinjuku-ku, Tokyo 160-8582, Japan*

*Author for correspondence (e-mail: awatabe@mail.ecc.u-tokyo.ac.jp)

Accepted 7 March 1005

Summary

Medaka genomic BAC clones, which contained two types of medaka hemopexin-like protein gene (*Wap65*), *mWap65-1* and *mWap65-2*, were screened and their genomic sequences were determined by the shotgun strategy. The exon–intron organizations were highly conserved between both *mWap65*s and human hemopexin genes. The 5′-flanking regions of *mWap65-1* and *mWap65-2* contained various putative transcription factor binding sites including elements for developmental regulation. The expression patterns of *mWap65*s during embryonic development were examined by quantitative real-time PCR, demonstrating that both *mWap65* transcripts were observed in early embryonic stages, but their expression patterns were different. Interestingly, *in situ* hybridization revealed that *mWap65-2* transcripts were restricted to liver, whereas *mWap65-1* transcripts were detected along the edge of pectoral fin buds and the median fin fold of tail buds in embryos at stage 32. Furthermore, we generated transgenic medaka expressing GFP driven by *mWap65-1* and *mWap65-2* promoters and observed GFP expression patterns during ontogeny. Although localizations of GFP varied among individuals, embryos uniformly expressed GFP 1 day after injection of *mWap65-1*-hrGFP and *mWap65-2*-hrGFP constructs, suggesting that *mWap65-1* and *mWap65-2* promoters were activated in very early stages. The differences between *mWap65-1* and *mWap65-2* in their expression profiles indicate their distinct roles during ontogeny.

Key words: medaka, *Oryzias latipes*, mWap65-1, mWap65-2, hemopexin, genomic sequences, embryo, gene expression, transgenic fish.

Introduction

Warm temperature acclimation-related 65 kDa protein, Wap65, was first identified as an abundant cytosolic protein in eurythermal fish such as carp *Cyprinus carpio* and goldfish *Carassius auratus* acclimated to 30°C (Kikuchi et al., 1993; Watabe et al., 1993). The highest accumulated levels of Wap65 mRNA have been observed in hepatopancreas and their deduced amino acid sequences resemble those of mammalian hemopexins (Kikuchi et al., 1995, 1997; Kinoshita et al., 2001). Hemopexin is a mammalian plasma glycoprotein that is mainly synthesized in liver, functioning as a scavenger of free heme with a high binding affinity to heme (Altruda et al., 1985; Nikkila et al., 1991; Morgan et al., 1993; Tolosano and Altruda, 2002). Crystal structural analysis of rabbit hemopexin revealed two essential histidine residues that are located at heme binding pockets (Paoli et al., 1999). Both carp and goldfish Wap65 lack one of the two essential histidine residues corresponding to heme axial ligands in hemopexins but the binding of Wap65 to heme had not been determined. Our recent study revealed the occurrence of two types of Wap65, mWap65-1 and mWap65-2 in medaka *Oryzias latipes* (Hirayama et al., 2004), and fWap65-1 and fWap65-2 in the pufferfish *Takifugu rubripes* (previously known as *Fugu rubripes*; Hirayama et al., 2003). Two types of Wap65-related protein also appear in the GenBank database for rainbow trout *Oncorhynchus mykiss* (Z68112 and AF281339), zebrafish *Danio rerio* (AI588537 and BM09558) and channel catfish *Ictalurus punctatus* (BM438553 and BM438613), suggesting that the duplication of the ancestral gene happened after teleosts and mammals had diverged. Although the two types of Wap65 from medaka and *Fugu* had primary structures similar to those of carp and goldfish, the expression patterns of *Wap65-1* and *Wap65-2* were not associated with variations in environmental temperatures (Hirayama et al., 2003, 2004). In terms of heme binding ability, mWap65-1 bound to heme despite lacking the two conserved histidine residues, whereas mWap65-2, with the two residues, did not (Hirayama et al., 2004). Therefore, structure–function relationships of the two types of Wap65 remain unclear.

Medaka is suitable for developmental and genetic studies as well as for transgenic experiments, because of the transparency

of the embryonic chorion, high fecundity and short generation times, in addition to its small genome size (Ishikawa, 2000; Gong et al., 2001). With such advantages, in this study we screened bacterial artificial chromosome (BAC) genomic clones from medaka containing the full-length sequences of *mWap65-1* and *mWap65-2*, determined their nucleotide sequences, including 5′- and 3′-flanking regions, and compared their genomic organizations with those of the human hemopexin gene. Then, we examined the expression profiles of *mWap65*s in medaka embryos using quantitative real-time PCR. Furthermore, we generated transgenic medaka expressing green fluorescent protein (GFP) driven by *mWap65-1* and *mWap65-2* promoters and observed their expression patterns during ontogeny.

Materials and methods

Materials

Adults of orange-red wild-type medaka *Oryzias latipes* Temminck and Schlegel, called himedaka, were fed *ad libitum* with commercial pellets and maintained at 25°C under the artificial conditions of 14 h:10 h light:dark.

Approximately 80 embryos incubated at 25°C were collected at each of the developmental stages: stage 9 [late morula stage, 7 h post-fertilization (hpf)], 13 (early gastrula stage, 14 hpf), 15 (mid gastrula stage, 19 hpf), 16 (late gastrula stage, 24 hpf), 18 (late neurula stage, 29 hpf), 20 (4 somite stage, 34 hpf), 22 (9 somite stage, 42 hpf), 24 (16 somite stage, 48 hpf), 28 (30 somite stage, 70 hpf), 36 (heart developmental stage, 156 hpf) and 39 (hatching stage, 240 hpf). Developmental stages were ascertained in a manner described by Iwamatsu (1994). Samples were frozen immediately in a liquid nitrogen bath and stored at –80°C until use for first strand cDNA synthesis.

Embryos at stage 32 (somite completion stage, 120 hpf) were collected and used for whole-mount *in situ* hybridization. For DNA microinjection, fertilized eggs were collected within 30 min after spawning and kept at 4°C to arrest development until microinjection.

Screening and sequencing of BAC clone

A BAC library of sperm genomic DNA from medaka of HNI strain and its high-density replica (HDR) filters has been constructed at Keio University School of Medicine, Japan (Kondo et al., 2002). The BAC library was screened by colony hybridization with both *mWap65*s probes. *mWap65-1* and *mWap65-2* probes were composed of 1096–1534 nucleotides (nt) and 838–1376 nt cDNAs (Hirayama et al., 2004), respectively, and labeled with digoxigenin (DIG)-11-dUTP using DIG-High Prime DNA Labeling and Detection Starter Kit II (Roche Diagnostics, Mannheim, Germany), according to the manufacturer's instruction. 1 μg of purified BAC DNAs from positive clones were digested with *Hin*dIII and separated on 0.7% agarose gels with a TBE buffer (0.089 mol l^{-1} Tris-borate, 0.5 mol l^{-1} EDTA). The digested DNAs were transferred to Biodyne B membranes (Pall BioSupport Division, Washington, NY, USA) and hybridized with the *mWap65-1* and *mWap65-2* probes by the method adopted for screening of the BAC library as described above.

Shotgun strategies were employed for sequencing selected clones, 182O24 including *mWap65-1* and 107E17 including *mWap65-2*. About 1150 and 1550 shotgun clones from BAC clones 182O24 and 107E17, respectively, were sequenced using ABI PRISM BigDye Cycle Terminator Ready Reaction Mix diluted with 5× sequencing buffer (Applied Biosystems, Foster City, CA, USA). Excess dye-terminators were removed by gel filtration and then PCR products were automatically loaded onto an ABI PRISM 377 or 3700 DNA analyzer (Applied Biosystems). To assemble the individual shotgun sequences into contigs, computer programs, Phred, Phrap and Consed were used for base calling, assembly of sequences, and viewing and editing analysis, respectively.

Analysis on genomic sequences

The exon–intron organizations of *mWap65-1* and *mWap65-2* were determined with genomic and cDNA nucleotide sequences (the DDBJ/EMBL/GenBank databases, accession numbers AB075198 for *mWap65-1* cDNA and AB075199 *mWap65-2* cDNA). The sequence of a 56 kb region containing 5′- and 3′-flanking sequences of *mWap65-1* with the coding sequence in the middle was compared with those of *mWap65-2* and the human hemopexin gene using the PipMaker (http://bio.cse.psu.edu/pipmaker/) (Schwartz et al., 2000) and RepeatMasker (Open-3.0 1996–2004; http://www.repeatmaster.org/; A. F. A. Smit, R. Hubley and P. Green, unpublished) (Smit and Green, 1999) programs. The human hemopexin gene had been mapped to chromosome 11p15.5-p15.4 (Law et al., 1988) and its sequence was obtained from NCBI's LocusLink (http://www.ncbi.nlm.nih.gov/genome/guide/human/). Putative *cis*-elements were searched by computer program TFSEARCH version 1.3 (http://www.cbrc.jp/research/db/TFSEARCH.html) that has been constructed for highly correlated sequence fragments in the TFMATRIX transcription factor binding site profile database in the TRANSFAC databases by GBF-Braunschweig (Heinemeyer et al., 1998).

Reverse transcription

Total RNA was extracted from embryos at various developmental stages using an ISOGEN system (Nippon Gene, Tokyo, Japan). To remove endogenous DNA contamination, the preparation containing total RNA was digested with DNase. An aliquot of 5 μg of total RNA was dissolved in 8.5 μl water and added with 5 U of DNase I (TaKaRa, Otsu, Japan) and 40 U of ribonuclease inhibitor (TaKaRa), then the RNA solution was incubated at 37°C for 1 h. The enzyme was inactivated at 98°C for 3 min, and the RNA solution was chilled on ice. First strand cDNA was synthesized as follows. One microlitre of 10 μmol l^{-1} adapter primer (5′-GGCCACGCGTCGACTAGTAC-3′), 2 μl of 10 mmol l^{-1} dNTP and 1 μl of water were added to the RNA solution treated with DNase. The reaction mixture was heated at 65°C for 5 min, quickly chilled on ice, added with 4 μl of 5× first-

strand buffer containing 250 mmol l^{-1} Tris-HCl (pH 8.3), 375 mmol l^{-1} KCl and 15 mmol l^{-1} $MgCl_2$, 0.1 mol l^{-1} dithiothreitol (DTT) and 200 U SuperScript™ III reverse transcriptase (Invitrogen, Carlsbad, CA, USA), and incubated at 42°C for 50 min. The enzyme was heat-inactivated at 70°C for 15 min and first strand cDNA synthesis was completed by treatment with 1.0 μl of RNase H (Invitrogen).

Real-time polymerase chain reaction (PCR) analysis

Primer pairs m1-F-1250 and m1-R-1319 for *mWap65-1*, m2-F-111 and m2-R-173 for *mWap65-2*, and m-bactin-F-7 and m-bactin-R-70 for medaka *β-actin* (Takagi et al., 1994) were designed using the Primer Express Software (Applied Biosystems) (Table 1). Each of 20 μl reaction mixtures contained 1× SYBR Green Master mix (Applied Biosystems), ≈25 ng of first strand cDNA and 8 pmol of each primer. Real-time PCR was performed with ABI PRISM 7300 (Applied Biosystems). Thermal cycling conditions consisted of the initial steps for 2 min at 50°C then 10 min at 95°C followed by 45 cycles of denaturation at 95°C for 15 s, annealing at 60°C for 1 min. Relative quantification was carried out by normalization the values relative to those of *β-actin*. Amplification specificity was examined using the melting curve following the manufacturer's instructions. Analysis and quantification using the comparative Ct method were carried out with the ABI Prism 7300 Sequence Detection Software (SDS) version 1.2 (Applied Biosystems).

Whole-mount in situ *hybridization*

Sense and antisense DIG-labeled RNA probes were synthesized from the DNA fragments of nt 1–1610 of *mWap65-1* cDNA and nt 96–1510 of *mWap65-2* cDNA with a DIG RNA labeling kit (Roche Diagnostics). DIG-labeling of RNA probes was carried out according to the manufacturer's instruction (Promega, Madison, WI, USA). Whole-mount *in situ* hybridization with the DIG-labeled RNA probes was performed according to the method of Westerfield (2000) with some modifications, as follows: after fixation at 4°C for 4 h in 4% paraformaldehyde in phosphate-buffered saline (PBS) containing 0.1% Tween 20 (PBSTw), the chorion was removed and embryos then refixed overnight at 4°C with the same solution. Treatment with proteinase K (TaKaRa; 5 μg ml l^{-1} in PBSTw) was carried out for 10 min at 37°C and the DIG-labeled RNA probes were used for hybridization at an approximate concentration of 1 μg ml l^{-1}.

Construction of recombinant GFP plasmids

mWap65-1 and *mWap65-2* upstream regions of ≈5 kb were amplified from BAC clones 182O24 and 107E17, respectively, by PCR using primers mWap65-1Fgfp5 and mWap65-1Rgfp5 for *mWap65-1* and mWap65-2Fgfp5 and mWap65-2Rgfp5 for *mWap65-2* (Table 2, Fig. 1). The amplified products of *mWap65-1* and *mWap65-2* were double-digested with *Bam*HI/*Hin*dIII and *Not*I/*Hin*dIII, respectively. The digested *mWap65-1* fragment was inserted into *Bam*HI and *Hin*dIII sites of the phrGFP vector (Stratagene, La Jolla, CA, USA), whereas that of *mWap65-2* was inserted into *Not*I and *Hin*dIII sites (Fig. 1). Plasmids of ≈8.5 kb, containing *mWap65-1* and *mWap65-2* upstream regions, were designated as *mWap65-1*-hrGFP and *mWap65-2*-hrGFP, respectively.

Microinjection

Microinjection was carried out according to the method of Kinoshita et al. (1996). A DNA solution of ≈20 ng μl^{-1} in distilled water was injected into the cytoplasm of blastomeres at the single cell stage. Eggs injected with recombinant GFP

Table 1. *Nucleotide sequences of primers used for quantitative real-time PCR*

Designation	Nucleotide sequence	Location*
m1-F-1250	5′-GAGCCCCAAAACCTTTGTAGCT-3′	1250–271
m1-R-1319	5′-GCCAAACAACTCCAGGGAAA-3′	1319–1338
m2-F-111	5′-TGCTTTTCTGGCCCTAATGC-3′	111–130
m2-R-173	5′-CCTGCTGCTGAATCCTCCAA-3′	173–192
m-bactin-F-7	5′-TCTGAGCGCCGTCACACA-3′	7–24
m-bactin-R-70	5′-CGTTTCAAGGGAATCGGTTTC-3′	70–90

*Numbers of nucleotides from the 5′- end of two types of *mWap65* and medaka *β-actin* cDNA. Two types of *mWap65* and medaka *β-actin* cDNA sequences were taken from Hirayama et al. (2004) and Takagi et al. (1994), respectively.

Table 2. *Nucleotide sequences of primers used for construction of* mWap65-1-*hrGFP and* mWap65-2-*hrGFP*

Designation	Nucleotide sequence	Location*
mwap65-1Fgfp5	5′-CGGGATCCGCGGAACTAGTGCTCTG-3′	–5021 to –5005
mwap65-1Rgfp5	5′-CCAAGCTTTGGTGTCCTCTGGTCCA-3′	–5 to –21
mwap65-2Fgfp5	5′-TTGCGGCCGCAGTGGCCAACTGTTACC-3′	–5080 to –5064
mwap65-2Rgfp5	5′-CCAAGCTTCCTGCGGAAATCTCTCC-3′	–23 to –7

*Numbers of nucleotides from the ATG initiation codon of two types of *mWap65* cDNA. Two types of *mWap65* cDNA sequences were taken from Hirayama et al. (2004).

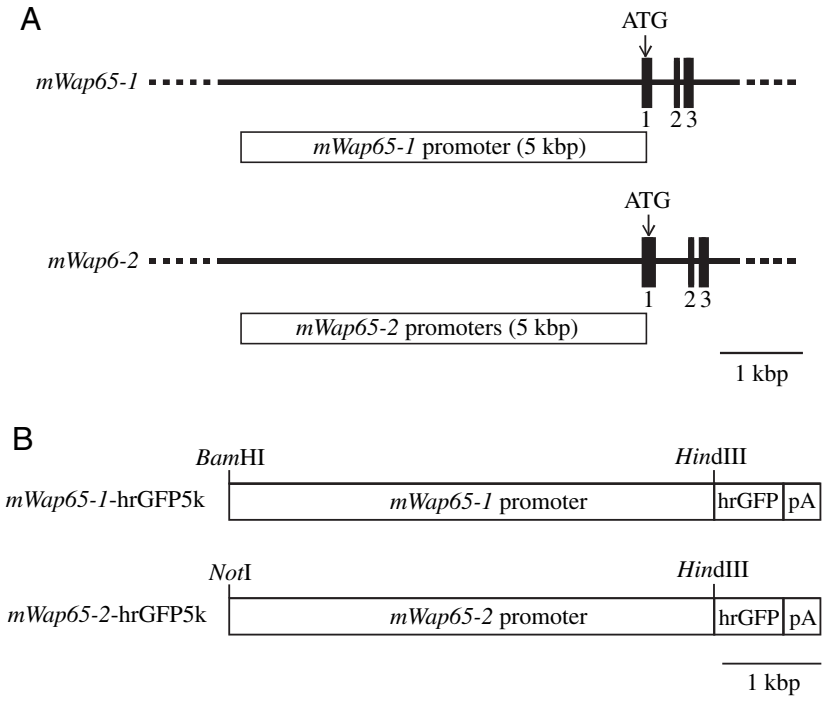

Fig. 1. Schematic representation of *mWap65-1*-hrGFP5k and *mWap65-2*-hrGFP5k constructs. (A) Structures of *mWap65-1* and *mWap65-2*. The initiation methionine codon (ATG) of *mWap65-1* and *mWap65-2* is located at 29 bp and 89 bp downstream the putative transcription start point, respectively. Promoters used in this study were DNA fragments of 5 kb in the 5′-flanking region for both *mWap65*s. Black boxes and lines indicate exons and introns, respectively. Numbers under the boxes indicate exon numbers from the 5′ end. (B) Structures of *mWap65-1*-hrGFP5k and *mWap65-2*-hrGFP5k constructs. DNA fragments of 5 kb in the 5′-flanking regions for both *mWap65*s were inserted into the phrGFP vector. pA, polyA signal.

plasmids were incubated at 25°C and GFP fluorescence was observed by fluorescence microscope.

Results

Characterization of genomic sequences of two medaka Wap65*s,* mWap65-1 *and* mWap65-2

An HNI strain genomic BAC library was screened to isolate *mWap65-1* and *mWap65-2*, resulting in isolation of two clones, 182O24 containing *mWap65-1* and 107E17 containing *mWap65-2*. The shotgun strategy revealed that the genomic BAC clones 182O24 and 107E17 contained 155 kb and 196 kb, respectively, whereas the sizes of *mWap65-1* and *mWap65-2* were 6.1 kb and 5.4 kb, respectively. The genomic nucleotide sequences of *mWap65-1* and *mWap65-2* have been registered in DDBJ/EMBL/GenBank with the accession numbers AB195240 and AB195241, respectively.

Exon-intron organizations were predicted using the genomic nucleotide sequences of *mWap65-1* and *mWap65-2*, and compared with that of the human hemopexin gene (Fig. 2). Both *mWap65*s consisted of 10 exons and 9 introns, as is the case for the human hemopexin gene. Although *mWap65*s were smaller than the human hemopexin gene (9.9 kb), their exon-intron organizations were almost identical.

The sequence of a 56 kb region containing 5′- and 3′-flanking sequences of *mWap65-1* with the coding sequence in the middle was compared with those of the corresponding regions of *mWap65-2* and the human hemopexin gene using the PipMaker program. As shown in Fig. 3, a high homology between *mWap65-1* and *mWap65-2* was found in the fifth,

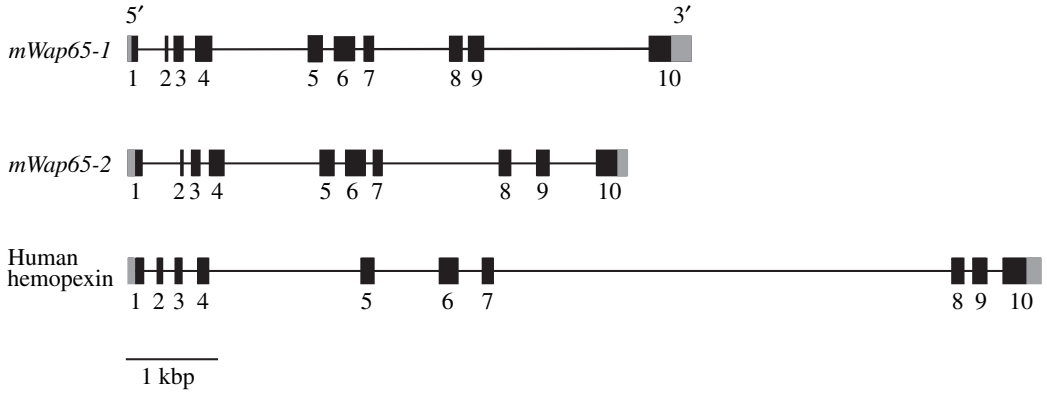

Fig. 2. Comparison of genomic organization of *mWap65-1* and *mWap65-2* with that of the human hemopexin gene. Exons, solid rectangles; introns, lines. Black and gray boxes indicate coding and non-coding regions, respectively. Numbers under the rectangles indicate the number of exons from the 5′ end. The genomic organization of the human hemopexin gene was constructed based on work by Takahashi et al. (1985), and the NCBI's LocusLink (http://www.ncbi.nlm.nih.gov/genome/guide/human/).

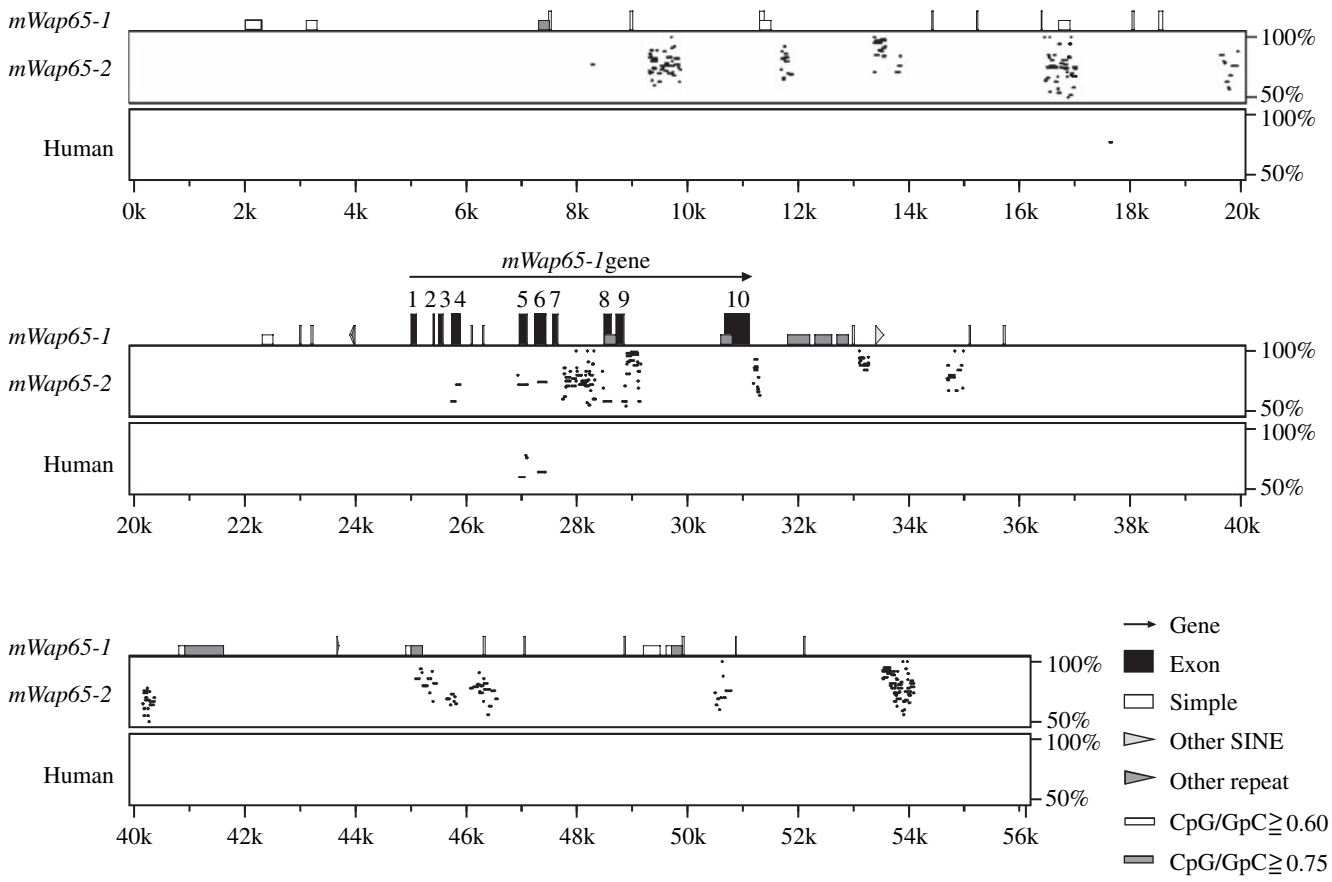

Fig. 3. PipMaker output comparison for *mWap65-1* with *mWap65-2* and the human hemopexin gene. Similarities of *mWap65-1* with *mWap65-2* and human hemopexin gene are shown on the vertical axis with percentages of sequence identity. The horizontal arrow indicates the direction of transcription. Exons are shown as tall black boxes; short white boxes represent CpG islands where the ratio CpG/GpC lies between 0.6 and 0.75; gray boxes represent ratios exceeding 0.75. Simple, simple repeat; SINE, short interspersed repetitive element.

sixth and eighth exons, and in the seventh and ninth introns. In the 5′- and 3′-flanking regions, homology was found 15.3 and 11.6 kb upstream and 2.1 and 22.5 kb downstream of the coding region of *mWap65-1*. *mWap65-1* showed an apparent homology with the human hemopexin gene only in the fifth and sixth exons (Fig. 3). *mWap65-1* also showed homology with *mWap65-2* and the human hemopexin gene in a very short sequence, considered to be a repetitive element.

Previously, Hirayama et al. (2004) determined the full-length of *mWap65-1* and *mWap65-2* cDNAs. In this study, we found that the sequences at the 5′ ends of the cDNA clones containing *mWap65-1* and *mWap65-2* were all identical (data not shown), and so the putative transcription start points of *mWap65*s were confirmed. Thus, putative transcription start points of *mWap65-1* and *mWap65-2* were located at 29 and 89 bases, respectively, upstream of the translation start site (Fig. 4). Putative *cis*-elements were searched using prediction programs. Although a 1 kb 5′-flanking region showed no obvious sequence homology among *mWap65-1*, *mWap65-2* and the human hemopexin gene (data not shown), various transcription factor binding sites known in vertebrates were found in mW*ap65*s (Fig. 4). The binding sites for HNF-3β, which is a liver-enriched transcription factor, were found at –344 for *mWap65-1* and –963 for *mWap65-2*. A Cdx1 binding site, which is an important element for developmental regulation (Subramanian et al., 1995), was abundant in the 5′-flanking regions of both *mWap65-1* (–790, –741, –672, –567, –471, –370, –307, –246) and *mWap65-2* (–940, –874, –812, –801, –793, –765, –707, –556, –539, –509, –494, –446, –339, –166). In addition, the 5′-flanking region of *mWap65-1* contained putative binding sites for SRY (–994, –532, –463, –343, –230, –155), USF (–854), Nkx-2.5 (–838, –687), MZF1 (–654, –201), Oct-1 (–516, –499), XFD-1 (–514), C/EBPα (–496), HFH-2 (–344), Evi-1 (–279), GATA-1 (–257) and AML-1a (–87), whereas that of *mWap65-2* consisted of SRY (–946, –500, –463, –419, –180, –89, –48), Pbx-1 (–837), Prx-2 (–861, –819), HFH-2 (–854), Nkx-2.5 (–815, –637, +58), XFD-1 (–778), δEF1 (–718), Brn-2 (–539), Oct-1 (–514), Sox-5 (–499), HNF-1 (–246) and c-Ets-1 (–72).

Real-time PCR analysis on expressional changes of mWap65-1 *and* mWap65-*2 during development*

Quantitative real-time RCR was performed to examine changes in the expression levels of *mWap65*s in embryos at

A *mWap65-1*

```
-1000 CAGTGAGGCTGTTCTGTAGCAACCCTGTACTCTGAAAGGTTGCTTCAGGATTCAGCCAGTGATCACGATT

-930  CTCTCAGTCTGACACCAGCAAATTGCACATCTAACATCTGTTTAATCGTGTTGTTAATGGTCATGTGACT
                                          SRY

-860  AATCACGCATGTGGATCTCAATTGAAGTGTTCTTCTGACTGTAGAAAAGAACATTGCTGGATATAATCTG
            USF          Nkx-2.5

-790  AATTAATTCATGTTGCCCTTTGTATCCATTGGATGAGGCCAACCCCCAAAATTCTGTTAATGTTCATCTG
      Cdx1                                              Cdx1

-720  AAGAACGTTATATAACCCAGGTTTGTGGAGATCTAAAGTGCACATGTCCACATTATTTGTCTATTTTGAG
                                 Nkx-2.5        Cdx1                    MZF1

-650  GGGACTCTGGGTTAGTTACCTTTGAGTTGAACCAGGCCTGAGCGGTAGACCGGGCAGACTTCCAGAAACC

-580  TCCGGAATCTACTTTTTATATACAAAGGTTGTAAAAAACATCAAAACAGTAGTTTATTTTGAAAAACATG
                  Cdx1                                SRY                Oct-1
                                                                         XFD-1

-510  TAAATATTAACGTCTGATTATGCAAAAACATTTGTCATTCATTAAAAAAAGAAAATGCCAAATTGTTGTA
                    Oct-1                          Cdx1      SRY
                              C/EBPα

-440  GGAGAAAATATATATCAATGTTGGGTCTCCAAAAGATGCTTTGCAGAAGTAATACAAACTATAGAACATG

-370  TAGAAATCCATTTTTAGGACTGTATAGTTTGTTTGTTTTTTAAGACTTTTAAAATGATTTTGCATAAAG
      Cdx1                        SRY                                  Cdx1
                                  HFH-2
                                  HNF-3β

-300  AGGCAGAAACATCTAAAGTCTACAAGATATCCATCTATTGATCAGACATCACGACAGAAATAAAGTTCAG
                          Evi-1                GATA-1      Cdx1

-230  TTTCTTTGAATTGCTGTGGGTGAGACATGGCTGGGGAGGGAGGATGGAGATCTCTGGGGGCACAATGTGG
      SRY                          MZF1

-160  GGGAAAATCAAACATCGTGGGTGTCTGACCAACGCCCTGCTCCTGCATGCTTGATCCCTCCTCCTTGGGC
            SRY

-90   GTCTGTGGTCCAATGTGAGGCTGCCTACATGGAGCGGCCGCTGATAAAAACGGATGGAGAGCTGGAGCCA
        AML-1a

-20   TGGCACCTTTCCCAGGATCTCCAGGCTTTGGACCAGAGGACACCACGAGATG
                                  +1
```

B *mWap65-2*

```
-1000 GACGCATTTTAAGCTGTGTTAAATAAAAAGTTAATACAAGTAAATAGTTGGACCCTTGTTTTTTTATACTT
                                  HNF-3β          SRY      Cdx1

-930  GAGAACACAACAAAAGTTATGGATTAAAAATGACGACGCCCTAAAAAAATAAAAAAAATAAATCAATAAA
                                                                  Pbx-1
                                                        Cdx1

-860  AAATTTAATTATTTTTTTTTTAAATCACACGCTTATTTGTCTGTACTTAATTAATTGCGATTAATGTGAT
            Prx-2                                 Prx-2                Cdx1  Cdx1
            HFH-2                                 Nkx-2.5
                                                  Cdx1

-790  AAATATCTCTGATATGTAAATAAAAAATAAATCAAGCACTGGGAGTAACAGCATCGAAAAACCCTAAATA
                  XFD-1      Cdx1

-720  ATTCACACCTAAATATAAATTGAATCCACGACCAAACGATACAAAAACGTGACTTATACTCTGGAAAATA
      δEF1       Cdx1

-650  TGGGGGACAGAAACTTAATAGCAAGGCTTCAAAGTCATTTGACAAGTTTTTCTTCTTTGAATACTTAAAA
                  Nkx-2.5

-580  GATCATACTTATGTTGGAATCATACATAATATTTTGTCTTTATTTATTACTTATGAATAAAATGTGGCAT
                        Cdx1                  Brn-2                      Oct-1
                                              Cdx1

-510  CATTACTATGAAAAACAATAATGCTTTGTAATCCTGCTAAACCAAGTGTTGTTTGCAGACACTACATTAA
      Cdx1          Cdx1                                SRY                Cdx1
                    Sox-5
                    SRY

-440  AAGTTGATTCAAGTTCAATTTTGTGTTTTCTGTCTATTGCAAATCTTCTCAATAAGACTTGAAAGTGTGT
                              SRY

-370  AGAGCAGATTTTAAGTACATTCACAAGACGCCATTAATGGGAAAATAAAGTCTGAGGAAGCAGTAAGAAA
                                    Cdx1

-300  AAGTGACACAATATGTCTTAAACTGACCAACGTGCAGCTATCAAACTTAAAAGGTGTAAAACATTAACCT
                                                                  HNF-1

-230  AATGGATCAATAGTACACTACATAGACTACCTTAAAGGGAACACAAAACATTTGTTTTTACCTAATTTAT
                                                  SRY                 Cdx1

-160  AACATGTTATTTCCAGCAAGTCATGCAGAGATTTTATCACAGATAACAGTGAATAATCTAAAATATTTGC

-90   ATTAGTTTTGTAACTGCAAAACTTCCAGTTCTTTCCCTGTGCAAACAAACACAGAAGGACACACACAGTT
        SRY                 c-Ets-1                 SRY

-20   TCCTAACATCCAGCCCACACAGATTTGAGGATAAAAGAGCATGTTAAGCTGCTGCATAGCTGCACTTCAC
                                  +1                                Nkx-2.5

      AGCTCTTTGCTCCAGTGGAGAGATTTCCGCAGGACAAGGATG
```

Fig. 4. The nucleotide sequences of 5′-flanking regions of *mWap65-1* (A) and *mWap65-2* (B). The nucleotide assigned +1 is the putative transcription start point. Putative transcription factor binding sites determined by TFSEARCH are underlined. SRY, sex determining region Y; USF, upstream stimulatory factor; Nkx-2.5, homeobox protein NK-2 homolog; Cdx1, caudal-type homeobox gene 1; MZF1, myeloid zinc finger 1; Oct-1, octamer-binding transcription factor 1; XFD-1, *Xenopus* fork head domain factor 1; C/EBPα, CCAAT/enhancer binding protein α; HFH-2, fork head homolog 2; HNF-3β, hepatocyte nuclear factor-3β; Evi-1, ectopic viral integration site 1 encoded factor 1; GATA-1, globin transcription factor-1; AML-1a, acute myeloid leukemia-1a; Pbx-1, pre-B-cell leukemia transcription factor-1; Prx-2, paired related homeobox 2; δEF1, δ-crystallin/E2-box factor 1; Brn-2, brain-2; Sox-5, SRY-related high mobility group protein (HMG)-box gene 5; HNF-1, hepatocyte nuclear factor 1; c-Ets-1, v-ets erythroblastosis virus E26 oncogene homolog 1.

stages 9-39, using those of *β-actin* as the internal standard. As shown in Fig. 5, the *mWap65-1* transcripts were detected in embryos at the beginning of the experiment, at stage 9, the late morula stage. The expression level at stage 13 (early gastrula) was about 30-fold higher than that at stage 9, and the highest expression level of *mWap65-1* was observed at stage 16 (late gastrula). Thereafter, the amount of transcripts was reduced at stages 18 (late neurula) to 24 (16 somite), but the expression level was increased again at stage 28, when 30 somites are formed in the trunk muscle, and almost constant levels of transcripts were maintained until hatching. In contrast, *mWap65-2* transcripts were not detected until stage 15 (mid gastrula) (Fig. 5). The *mWap65-2* transcripts were first observed at stage 16. Then the expression levels were rapidly increased until hatching, although the levels were slightly decreased at stage 24 (16 somite) compared with those at stage 22 (9 somite). Thus, expression patterns of *mWap65-1* and *mWap65-2* were markedly different from each other.

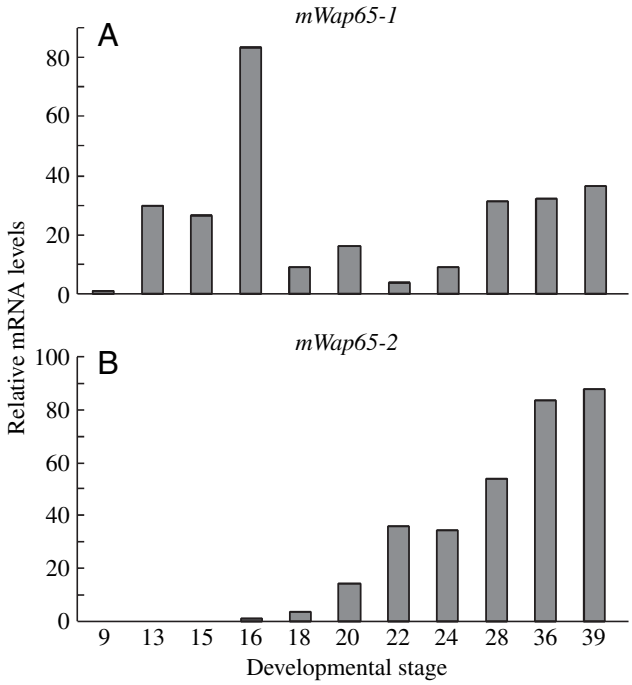

Fig. 5. Changes in the relative accumulated mRNA levels of *mWap65-1* (A) and *mWap65-2* (B) in medaka embryos during development. Total RNAs were isolated from embryos at various stages of 9 to 39. The relative levels were determined using those of *β-actin* as the control. The values were expressed as the ratios to the lowest value obtained in this study.

Spatial expression patterns of mWap65-1 *and* mWap65-2 *in medaka embryos*

To examine spatial expression patterns of *mWap65*s, whole-mount *in situ* hybridization was performed on embryos at stage 32, at which point somite formation is complete. *mWap65-1* hybridization signals were observed along the edge of pectoral fin bud and median fin fold of the tail bud, but not in the liver (Fig. 6). However, *mWap65-2* was observed only in liver, clearly demonstrating different functions of *mWap65-1* and *mWap65-2* during ontogeny. No signal was detected with sense probes for *mWap65*s (data not shown).

Expression of GFP in embryos injected with mWap65-1-*hrGFP and* mWap65-2-*hrGFP constructs*

mWap65-1-hrGFP and *mWap65-2*-hrGFP constructs were injected into embryos at the single cell stage. One day after injection with the *mWap65-1*-hrGFP construct, GFP fluorescence spots were observed throughout the blastoderm including the embryonic shield, when embryos attained stage 16 (late gastrula) (Fig. 7A). Following development from stage 16 to stage 29, GFP fluorescence was observed not only in yolk sac but also various areas of the embryonic body. Large and many small fluorescent spots were observed in the yolk sac at stages 23 (12 somite; Fig. 7C) and 26 (22 somite; Fig. 7E) as

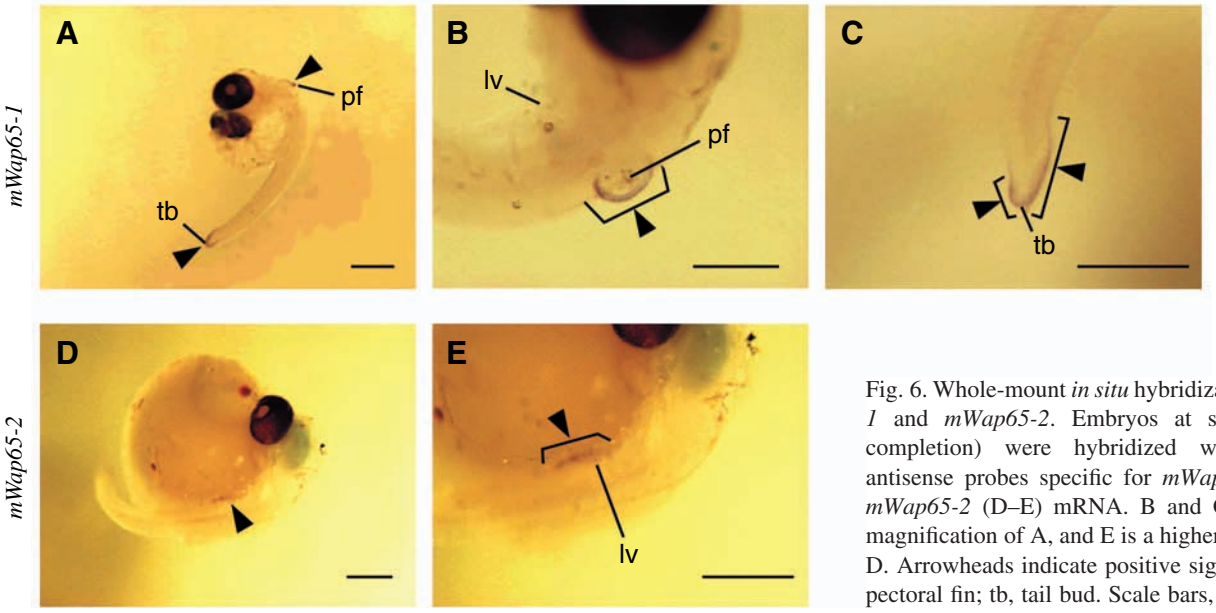

Fig. 6. Whole-mount *in situ* hybridization of *mWap65-1* and *mWap65-2*. Embryos at stage 32 (somite completion) were hybridized with DIG-labeled antisense probes specific for *mWap65-1* (A–C) and *mWap65-2* (D–E) mRNA. B and C show a higher magnification of A, and E is a higher magnification of D. Arrowheads indicate positive signals. lv, liver; pf, pectoral fin; tb, tail bud. Scale bars, 240 μm.

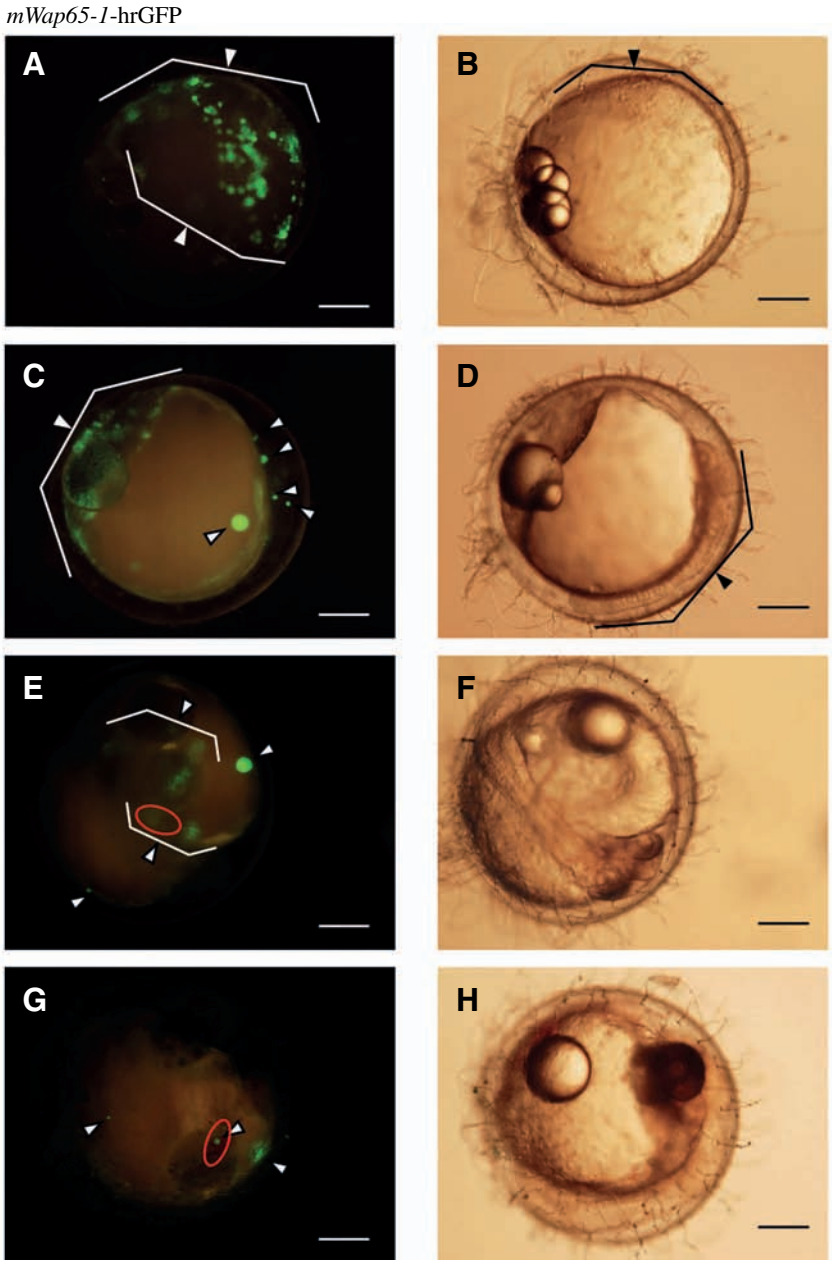

Fig. 7. Transient expression of GFP in medaka embryos injected with *mWap65-1*-hrGFP5k construct and examined under dark-field (A,C,E,G) and light-field (B,D,F,H) optics. (A,B) Stage 16 (late gastrula); (C,D) stage 23 (12 somite); (E,F) stage 26 (22 somite); (G,H) stage 29 (34 somite). White arrowheads indicate cells showing GFP fluorescence. Embryonic shield and body (outlined) are shown with black arrowheads. Red lines surround liver anlage. Scale bars, 240 μm.

well as in the embryonic body (Fig. 7C, right part). However, the small fluorescent spots tended to disappear at stage 26 and in turn a new fluorescent spot was found in the area of the liver anlage, a primitive form of liver in embryos (Fig. 7E). The fluorescence of liver anlage was more clearly observed in the embryo at stage 29 (Fig. 7G).

Embryos injected with the *mWap65-2*-hrGFP construct expressed GFP at stage 16 (Fig. 8A), as was the case with *mWap65-1*. At this stage also fluorescent spots of *mWap65-2*-hrGFP were again observed in various areas of the blastoderm, including the embryonic shield. Similarly to the expression patterns of *mWap65-1*-hrGFP, the *mWap65-2*-hrGFP fluorescent spots mostly disappeared at stage 26. However, *mWap65-2*-hrGFP was first observed in liver anlage in the embryos at stage 30 (35 somite) (Fig. 8E) in contrast to *mWap65-1*-hrGFP, which was activated in this tissue as early as at stage 26 (22 somite). These differences in expression patterns between *mWap65-1*-hrGFP and *mWap65-2*-hrGFP appeared to reflect those of the accumulated mRNA levels as shown in Fig. 5. Although *mWap65-1*-hrGFP was examined for its activation profiles until hatching, an intense GFP fluorescence was observed only in liver (Fig. 9).

Discussion

We determined the nucleotide sequences of BAC clones containing genomic sequences of two medaka *Wap65*s, *mWap65-1* and *mWap65-2*. Recently we have characterized two *Fugu Wap65*s, *fWap65-1* and *fWap65-2*, and demonstrated that exon–intron organizations were conserved among *fWap65-1*, *fWap65-2* and the human hemopexin gene (Hirayama et al., 2003). Both *mWap65*s in this study consisted of 10 exons and 9 introns (see Fig. 2) as is the case in the human hemopexin gene and *fWap65*s.

Alignment of nucleotide sequences using the PipMaker program revealed that not only *fWap65-1* (Hirayama et al., 2003) but also *mWap65-1* showed apparent homology with the human hemopexin gene in the fifth and sixth exons (see Fig. 3). These encode a potential receptor binding site, by which rabbit hemopexin is bound to hepatoma cells (Morgan et al., 1988, 1993). It has been reported for rabbit hemopexin that eight hydrophobic residues are important in the structural stability around the heme binding site (Paoli et al., 1999). In the case of *Fugu*, fWap65-1 contained five, and fWap65-2 seven, out of the eight hydrophobic residues found in rabbit hemopexin and most of these residues were located in the sixth exon. These residues were also found in mWap65s (data not shown), suggesting their importance in structural integrity.

No apparent sequence homology was found in the 5′-flanking region 1 kb upstream the coding sequence among *mWap65-1*, *mWap65-2* and human hemopexin gene. However, this region was found to contain various transcription factor

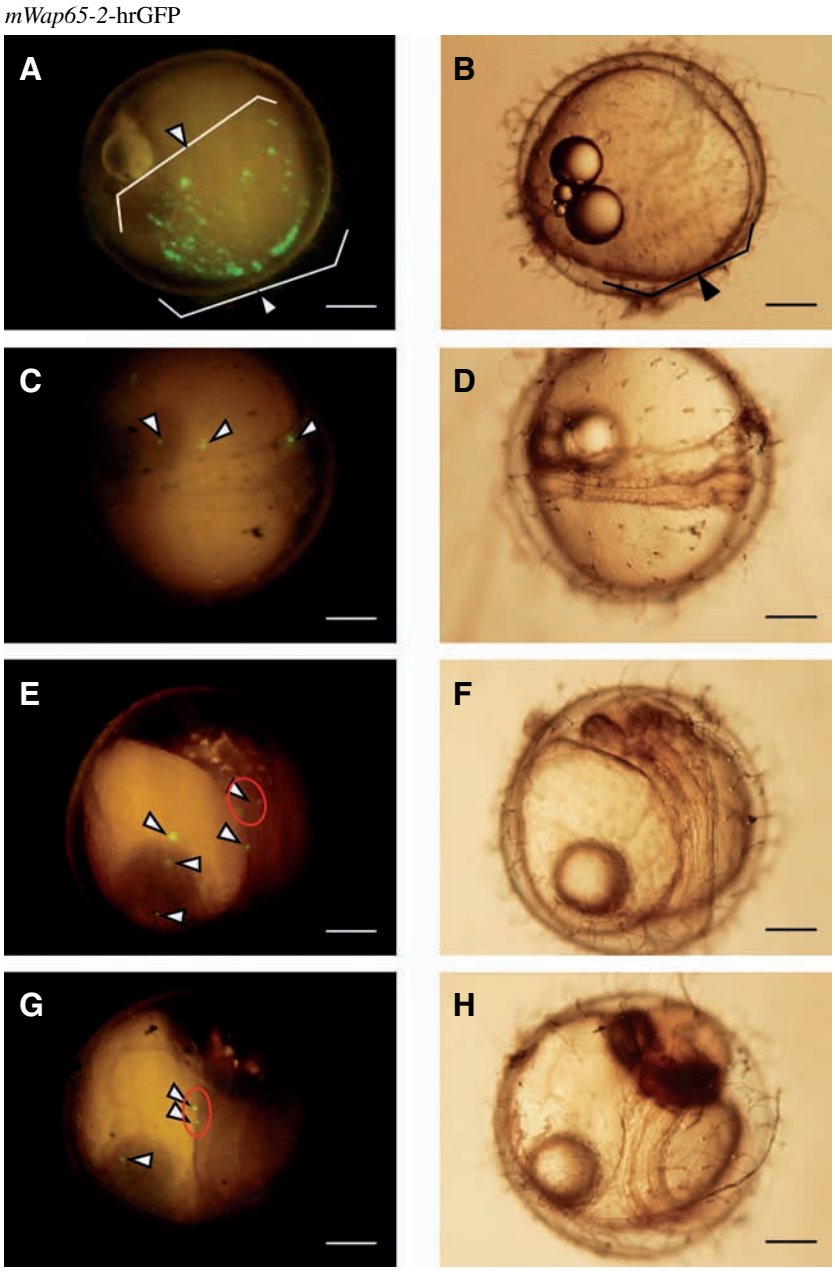

Fig. 8. Transient expression of GFP in medaka embryos injected with *mWap65-2*-hrGFP5k construct. (A,B) Stage 16 (late gastrula); (C,D) stage 26 (22 somite); (E,F) stage 30 (35 somite); (G,H) stage 31 (gill blood vessel formation). Transgenic embryos were exposed under dark- (A,C,E,G) and light-field illumination (B,D,F,H). White arrowheads indicate cells showing GFP fluorescence. Embryonic shield is indicated by a black arrowhead. Red lines surround liver anlage. Scale bars, 240 μm.

binding sites (see Fig. 4). Interestingly, several transcriptional elements, which are thought to regulate development, are contained in both *mWap65*s. While Cdx1 is considered to be a regulator of Hox gene expression (Subramanian et al., 1995), putative binding sites for Cdx1 are rich in the 5′-flanking regions of both *mWap65*s. Found also in *mWap65*s were the binding sites for Nkx-2.5, a vertebrate homologue of tinman from *Drosophila melanogaster* involved in cardiac mesoderm formation (Bodmer et al., 1990; Lints et al., 1993), and Prx-2, a homeobox transcription factor possibly playing roles in development of the heart and forebrain (Leussink et al., 1995), as in the case of *fWap65*s (Hirayama et al., 2003). The presence of these binding sites in the 5′-flanking regions of *Wap65*s indicates their involvement in the transcriptional regulation during development.

Rat hemopexin transcripts were first detected in liver on day 24 of gestation and rapidly increase during the postnatal period (Nikkila et al., 1991). Chicken hemopexin is found around hatching and increases in 4-day-old chicken to more than 1000-fold over embryonic levels as revealed by electroimmunoassay of serum (Grieninger et al., 1986).

Quantitative real-time PCR in this study revealed that *mWap65-1* transcripts were detected even at stage 9, the beginning of the experiments (see Fig. 5). Our previous study showed that *mWap65-1* transcripts were first detected at stage 24 by semi-quantitative RT–PCR (Hirayama et al., 2004). Interestingly, quantitative real-time PCR analysis showed that embryos expressed *mWap65-1* transcripts even when embryonic shield was not observed, and their maximum levels were observed in embryos at stage 16, when the blastoderm covers three-quarters of the yolk sphere and the embryonic shield becomes evident (Iwamatsu, 1994). The embryonic shield is formed at stage 16, followed by the formation of somite, notochord and organs until hatching. The high expression levels of *mWap65-1* in early embryonic stages indicate a possible role of this gene in early embryogenesis.

mWap65-2 transcripts were first detected at stage 16 and thereafter gradually increased during ontogeny, as embryos undergo dynamic changes of their morphology. These results, together with the presence of putative transcriptional elements involving development in the 5′-flanking region of *mWap65-2*, suggests that *mWap65-2* also plays important roles in embryonic development.

Medaka embryos injected with *mWap65-1*-hrGFP- and *mWap65-2*-hrGFP expressed GFP fluorescence at stage 16, 1 day after injection, suggesting that *mWap65-1* and *mWap65-2* promoters were both activated at early developmental stages. Such GFP expression in the early embryonic stages was consistent with the results obtained by real-time RT-PCR (Fig. 5).

mWap65-2 transcripts were expressed in liver as revealed by *in situ* hybridization (see Fig. 6). Unexpectedly, those of *mWap65-1* were expressed along the edge of pectoral fin bud

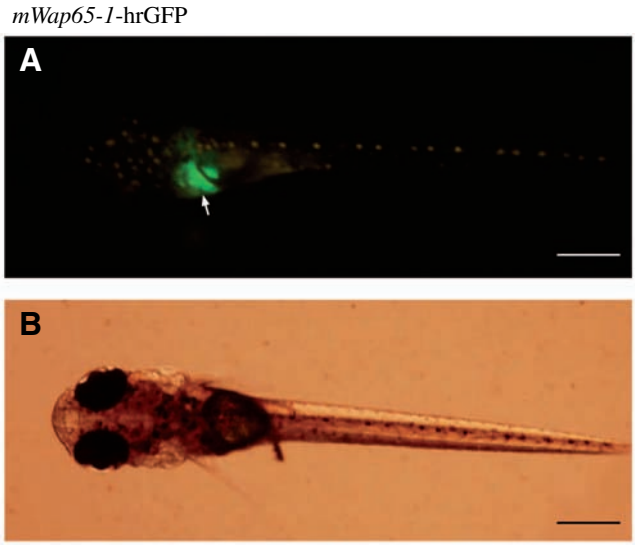

Fig. 9. Transient expression of GFP in the medaka larva after hatching (11 days post-fertilization), which had been injected with the *mWap65-1*-hrGFP5k plasmid. (A) Dark-field and (B) light-field illumination. Arrow indicates liver. Scale bars, 450 μm.

and median fin fold of the tail bud in embryos at stage 32, suggesting a function of *mWap65-2* in the development of these two tissues. GFP fluorescence was restricted to the liver of hatched medaka injected with *mWap65-1*-hrGFP (see Fig. 9), shifting its localization during hatching. While the *msx* homeobox genes are known to be important for limb development in mouse (Muneoka and Sasoon, 1992), their homologs are expressed in zebrafish embryos along the edge of the pectoral fin bud and median fin fold of the tail bud during development (Akimenko et al., 1995).

We observed transient expression profiles of GFP driven by two *mWap65*s promoter in this study, but the localization of expressed GFP varied among individuals (data not shown). It is known that the F_0 generation of transgenic fish show the mosaic expression patterns of transgenes (Ju et al., 1999) and the uniform expression of transgenes is normally attained in the F_1 or F_2 generation (Chou et al., 2001). We are now generating stable transgenic lines to reveal more precisely the spatiotemporal expression patterns of *mWap65*s.

In conclusion, we determined the genomic nucleotide sequences of two *mWap65*s and their flanking sequences. Furthermore, the expression profiles of *mWap65*s were determined using quantitative real-time PCR and *in situ* hybridization. We also generated transgenic medaka expressing GFP driven by two *mWap65* promoters, and examined their expression patterns. The spatiotemporal patterns in embryos were different between *mWap65-1* and *mWap65-2*, suggesting their distinct roles, at least during ontogeny.

We would like to thank T. Watanabe, The University of Tokyo, for his technical assistance. This study was partly supported by a Grant-in-Aid from the Ministry of Education, Culture, Sports, Science and Technology of Japan.

References

Akimenko M. A., Johnson, S. L., Westerfield, M. and Ekker, M. (1995). Differential induction of four *msx* homeobox genes during fin development and regeneration in zebrafish. *Development* **121**, 347-357.

Altruda, F., Poli, V., Restagno, G., Argos, P., Cortese, R. and Silengo, L. (1985). The primary structure of human hemopexin deduced from cDNA sequence: evidence for internal, repeating homology. *Nucleic Acids Res.* **13**, 3841-3859.

Bodmer, R., Jan, L. Y. and Jan, Y. N. (1990). A new homeobox-containing gene, *msh-2*, is transiently expressed early during mesoderm formation in *Drosophila*. *Development* **110**, 661-669.

Chou, C. Y., Horng, L. S. and Tsai, H. J. (2001). Uniform GFP-expression in transgenic medaka (*Oryzias latipes*) at the F0 generation. *Transgenic Res.* **10**, 303-315.

Gong, Z., Ju, B. and Wan, H. (2001). Green fluorescent protein (GFP) transgenic fish and their applications. *Genetica* **111**, 213-225.

Grieninger, G., Liang, T. J., Beuving, G., Goldfarb, V., Metcalfe, S. A. and Muller-Eberhard, U. (1986). Hemopexin is a developmentally regulated, acute-phase plasma protein in the chicken. *J. Biol. Chem.* **261**, 15719-15724.

Heinemeyer, T., Wingender, E., Reuter, I., Hermjakob, H., Kel, A. E., Kel, O. V., Ignatieva, E. V., Ananko, E. A., Podkolodnaya, O. A., Kolpakov, F. A. et al. (1998). Databases on transcriptional regulation: TRANSFAC, TRRD and COMPEL. *Nucleic Acids Res.* **26**, 362-367.

Hirayama, M., Nakaniwa, M., Ikeda, D., Hirazawa, N., Otaka, T., Mitsuboshi, T., Shirasu, K. and Watabe, S. (2003). Primary structures and gene organizations of two types of Wap65 from the pufferfish *Takifugu rubripes*. *Fish Physiol. Biochem.* **29**, 211-224.

Hirayama, M., Kobiyama, A., Kinoshita, S. and Watabe, S. (2004). The occurrence of two types of hemopexin-like protein in medaka and differences in their affinity to heme. *J. Exp. Biol.* **207**, 1387-1398.

Ishikawa, Y. (2000). Medakafish as a model system for vertebrate developmental genetics. *BioEssays* **22**, 487-495.

Iwamatsu, T. (1994). Stages of normal development in the medaka *Oryzias latipes*. *Zool. Sci.* **11**, 825-839.

Ju, B., Xu, Y., He, J., Liao, J., Yan, T., Hew, C. L., Lam, T. J. and Gong, Z. (1999). Faithful expression of green fluorescent protein (GFP) in transgenic zebrafish embryos under control of zebrafish gene promoters. *Dev. Genet.* **25**, 158-167.

Kikuchi, K., Watabe, S., Suzuki, Y., Aida, K. and Nakajima, H. (1993). The 65-kDa cytosolic protein associated with warm temperature acclimation in goldfish, *Carassius auratus*. *J. Comp. Physiol. B* **163**, 349-354.

Kikuchi, K., Yamashita, M., Watabe, S. and Aida, K. (1995). The warm temperature acclimation-related 65-kDa protein, Wap65, in goldfish and its gene expression. *J. Biol. Chem.* **270**, 17087-17092.

Kikuchi, K., Watabe, S. and Aida, K. (1997). The Wap65 gene expression of goldfish (*Carassius auratus*) in association with warm water temperature as well as bacterial lipopolysaccharide (LPS). *Fish Physiol. Biochem.* **17**, 423-432.

Kinoshita, M., Toyohara, H., Sakaguchi, M., Inoue, K., Yamashita, S., Satake, M., Wakamatsu, Y. and Ozato, K. (1996). A stable line of transgenic medaka (*Oryzias latipes*) carrying the CAT gene. *Aquaculture* **143**, 267-276.

Kinoshita, S., Itoi, S. and Watabe, S. (2001). cDNA cloning and characterization of the warm-temperature-acclimation-associated protein Wap65 from carp, *Cyprinus carpio*. *Fish Physiol. Biochem.* **24**, 125-134.

Kondo, M., Froschauer, A., Kitano, A., Nanda, I., Hornung, U., Volff, J. N., Asakawa, S., Mitani, H., Naruse, K., Tanaka, M. et al. (2002). Molecular cloning and characterization of *DMRT* genes from the medaka *Oryzias latipes* and the platyfish *Xiphophorus maculatus*. *Gene* **295**, 213-222.

Law, M. L., Cai, G. Y., Hartz, J. A., Jones, C. and Kao, F. T. (1988). The hemopexin gene maps to the same location as the β-globin gene cluster on human chromosome 11. *Genomics* **3**, 48-52.

Leussink, B., Brouwer, A., El Khattabi, M., Poelmann, R. E., Gittenberger-de Groot, A. C. and Meijlink, F. (1995). Expression patterns of the paired-related homeobox genes *MHox/Prx1* and *S8/Prx2* suggest roles in development of the heart and the forebrain. *Mech. Dev.* **52**, 51-64.

Lints, T. J., Parsons, L. M., Hartley, L., Lyons, I. and Harvey, R. P. (1993). *Nkx-2.5*: a novel murine homeobox gene expressed in early heart progenitor cells and their myogenic descendants. *Development* **119**, 419-431.

Morgan, W. T., Muster, P., Tatum, F. M., McConnell, J., Conway, T. P., Hensley, P. and Smith, A. (1988). Use of hemopexin domains and monoclonal antibodies to hemopexin to probe the molecular determinants of hemopexin-mediated heme transport. *J. Biol. Chem.* **263**, 8220-8225.

Morgan, W. T., Muster, P., Tatum, F. M., Kao, S. M., Alam, J. and Smith, A. (1993). Identification of the histidine residues of hemopexin that coordinate with heme-iron and of a receptor-binding region. *J. Biol. Chem.* **268**, 6256-6262.

Muneoka, K. and Sassoon, D. (1992). Molecular aspects of regeneration in developing vertebrate limbs. *Dev. Biol.* **152**, 37-49.

Nikkila, H., Gitlin, J. D. and Muller-Eberhard, U. (1991). Rat hemopexin. Molecular cloning, primary structural characterization, and analysis of gene expression. *Biochemistry* **30**, 823-829.

Paoli, M., Anderson, B. F., Baker, H. M., Morgan, W. T., Smith, A. and Baker, E. N. (1999). Crystal structure of hemopexin reveals a novel high-affinity heme site formed between two β-propeller domains. *Nature Struct. Biol.* **6**, 926-931.

Schwartz, S., Zhang, Z., Frazer, K. A., Smit, A., Riemer, C., Bouck, J., Gibbs, R., Hardison, R. and Miller, W. (2000). PipMaker – a web server for aligning two genomic DNA sequences. *Genome Res.* **10**, 577-586.

Subramanian, V., Meyer, B. I. and Gruss, P. (1995). Disruption of the murine homeobox gene *Cdx1* affects axial skeletal identities by altering the mesodermal expression domains of *Hox* genes. *Cell* **83**, 641-653.

Takagi, S., Sasado, T., Tamiya, G., Ozato, K., Wakamatsu, Y., Takeshita, A. and Kimura, M. (1994). An efficient expression vector for transgenic medaka construction. *Mol. Mar. Biol. Biotechnol.* **3**, 192-199.

Takahashi, N., Takahashi, Y. and Putnam, F. W. (1985). Complete amino acid sequence of human hemopexin, the heme-binding protein of serum. *Proc. Natl. Acad. Sci. USA* **82**, 73-77.

Tolosano, E. and Altruda, F. (2002). Hemopexin: structure, function, and regulation. *DNA Cell Biol.* **21**, 297-306.

Watabe, S., Kikuchi, K. and Aida, K. (1993). Cold- and warm-temperature acclimation induces specific cytosolic proteins in goldfish and carp. *Nippon Suisan Gakkaishi* **59**, 151-156.

Westerfield, M. (2000). *The Zebrafish Book. A Guide for the Laboratory Use of Zebrafish (*Danio rerio*)*, 4th edn. Eugene, Oregon, USA: University of Oregon Press.